INTERNATIONAL JOURNAL OF PHARMACEUTICAL SCIENCES
[ISSN: 0975-4725; CODEN(USA): IJPS00]
Journal Homepage: https://www.ijpsjournal.com

OPEN ACCESS

**Review Article**

# Identification of Novel Inhibitors Targeting Inflammatory Pathways in Rheumatoid Arthritis through Drug Design, Computational Docking, and Prediction Studies

**Ravi Kant Kushwaha*, Santosh Kumar Yadav, Alok Saini**

*Maharishi University of Information Technology, Lucknow*

ARTICLE INFO

Published: 10 Aug 2026
Keywords:
Rheumatoid Arthritis, Molecular Docking, TNF-α Inhibition, JAK3 Kinase, ADME and Toxicity Prediction.
DOI:
10.5281/zenodo.21874491

## ABSTRACT

Rheumatoid arthritis (RA) is a progressive autoimmune condition marked by chronic inflammation and joint damage, largely driven by molecular players like TNF-α and JAK3. In an effort to uncover potential therapeutic leads, this study focused on evaluating a set of fifteen naturally derived and synthetic compounds through molecular docking techniques. The docking analyses were carried out using the crystal structures of TNF-α (PDB ID: 6RMJ) and JAK3 kinase (PDB ID: 3LXK). Notably, compounds such as 2-(1-phenylethyl) phenol and select flavonoid derivatives showed favorable binding scores, indicating a potential to interfere with these inflammatory mediators. To further assess the viability of these candidates, we performed ADME profiling and toxicity predictions using SwissADME and ProTox-II. The findings revealed that most top-performing compounds had acceptable physicochemical properties, reasonable water solubility, and limited predicted toxicity. However, some limitations were observed, including low gastrointestinal absorption in certain flavonoids and mild enzyme inhibition risks. Overall, this computational approach highlights a promising direction for early-stage drug discovery in RA, with several compounds standing out as strong candidates for further refinement and experimental validation.

## INTRODUCTION

Rheumatoid arthritis (RA) is a chronic systemic autoimmune disease characterized by persistent synovial inflammation, progressive cartilage destruction, bone erosion, and joint deformity, ultimately leading to pain, functional disability, and reduced quality of life (1). RA affects approximately 0.5–1% of the global population, with a higher prevalence among women and older adults, and continues to represent a major healthcare burden worldwide (2). The pathogenesis of RA is driven by a complex interplay between genetic susceptibility,

***Corresponding Author:** Ravi Kant Kushwaha
**Address:** *Maharishi University of Information Technology, Lucknow*
**Email** ✉: santoshc25656@gmail.com
**Relevant conflicts of interest/financial disclosures**: The authors declare that the research was conducted in the absence of any commercial or financial relationships that could be construed as a potential conflict of interest.

environmental factors, and dysregulated immune responses.(3) Activated immune cells within the synovial membrane produce excessive levels of pro-inflammatory cytokines, particularly tumor necrosis factor-alpha (TNF-α) and other inflammatory mediators, which stimulate chronic inflammation and activate intracellular signaling pathways such as the Janus kinase/signal transducer and activator of transcription (JAK/STAT) pathway (4)(5). Persistent activation of these signaling cascades promotes synovial hyperplasia, pannus formation, cartilage degradation, and bone destruction, making TNF-α and JAK3 attractive therapeutic targets for the treatment of RA.(6) Current therapeutic strategies for RA include non-steroidal anti-inflammatory drugs (NSAIDs), corticosteroids, conventional disease-modifying antirheumatic drugs (DMARDs), biologic DMARDs targeting TNF-α, and targeted synthetic DMARDs such as JAK inhibitors. Although these therapies have significantly improved disease management, their long-term clinical use is of therapeutic resistance (7,8). Consequently, the discovery of novel anti-inflammatory agents with improved efficacy, selectivity, and safety remains an important objective in RA drug development. Recent advances in computer-aided drug design (CADD) have greatly accelerated the identification of potential drug candidates by enabling rapid virtual screening and prediction of ligand–protein interactions before experimental evaluation.(9) Among these computational approaches, molecular docking has become a widely used technique for estimating binding affinity, predicting binding modes, and understanding the molecular interactions responsible for biological activity (10,11). When combined with absorption, distribution, metabolism, and excretion (ADME) profiling and toxicity prediction, molecular docking provides a reliable and cost-effective strategy for prioritizing promising lead compounds for further biological evaluation.(12) Phenolic compounds and flavonoids have attracted considerable attention because of their broad spectrum of biological activities, including antioxidant, anti-inflammatory, and immunomodulatory effects (13). Numerous studies have demonstrated that these natural scaffolds can regulate inflammatory signaling pathways and suppress the production of pro-inflammatory mediators, suggesting their potential as lead molecules for the development of novel anti-rheumatoid agents (14,15) Structural modification of these compounds further provides opportunities to improve their pharmacological and physicochemical properties.

Therefore, the present study aimed to identify potential inhibitors of key inflammatory targets involved in RA by computational approaches. A total of fifteen naturally derived and synthetic phenolic and flavonoid compounds were selected and evaluated against TNF-α (PDB ID: 6RMJ) and Janus kinase 3 (JAK3; PDB ID: 3LXK) using molecular docking. The most promising compound was subsequently subjected to ADME and ProTox-II toxicity prediction to assess its pharmacokinetic characteristics and safety profile(16,17) The findings of this study provide valuable insights into the identification of novel lead molecules targeting inflammatory pathways and establish a computational basis for the future development of safer and more effective therapeutic agents for rheumatoid arthritis.

## 2. METHODOLOGY AND METHODS

### 2.1. Natural Compound Selection

A total of 15 natural compounds were selected from the literature based on their reported anti-inflammatory and antioxidant activities. The selected compounds primarily belong to the phenolic and flavonoid classes and were chosen

for their potential to interact with inflammatory targets implicated in rheumatoid arthritis. The two-dimensional (2D) chemical structures of all selected compounds were drawn using ChemDraw, and their molecular formulas were verified before subsequent computational analyses.(18) The complete list of compounds, along with their molecular formulas and chemical structures, is presented in Table 1

**Table 1: Chemical structures and molecular formulas of the selected compounds.**

| Sr. No. | Compounds | Molecular formula | Structure |
|---|---|---|---|
| 1 | ortho-benzylphenols | $C_{13}H_{12}O$ | 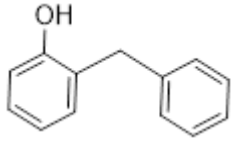 |
| 2 | 3,4-dimethylphenol | $C_8H_{10}O$ | 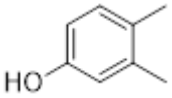 |
| 3 | para-cresol | $C_7H_8O$ | 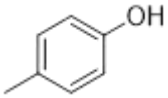 |
| 4 | 2-(1-phenylethyl) phenol | $C_{14}H_{14}O$ | 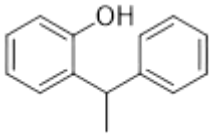 |
| 5 | 2-methyl-6-(1-phenylethyl) phenol | $C_{15}H_{16}O$ | 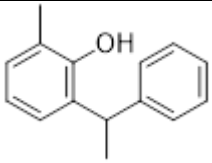 |
| 6 | 4,5-dimethyl-2-(1-phenylethyl) phenol | $C_{16}H_{18}O$ | 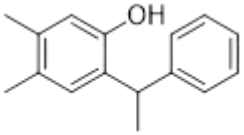 |
| 7 | 2-chloro-6-(1-phenylethyl) phenol | $C_{14}H_{13}ClO$ | 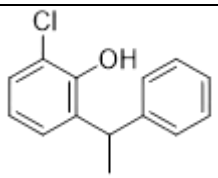 |
| 8 | 4-ethyl-2-(1-phenylethyl) phenol | $C_{16}H_{18}O$ | 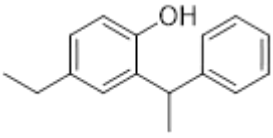 |
| 9 | 4-methyl-2-(1-phenylethyl) phenol | $C_{84}H_{90}O_4$ | 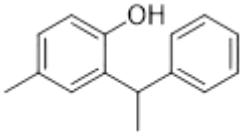 |
| 10 | para-fluorophenol | $C_6H_5FO$ | 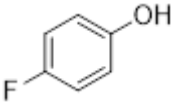 |
| 11 | ortho-benzylated phenols | $C_{13}H_{11}ClO$ | 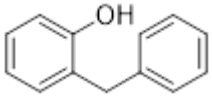 |

| | | | |
|---|---|---|---|
| 12 | 3,5,7-trihydroxy-2-(4-hydroxyphenyl)-4H-chromen-4-one | $C_{15}H_{10}O_6$ | 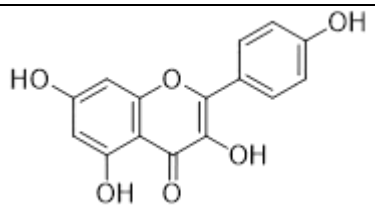 |
| 13 | 3,5,7-Trihydroxy-2-(3,4,5-trihydroxyphenyl)-4H-1-benzopyran-4-one | $C_{15}H_{10}O_8$ | 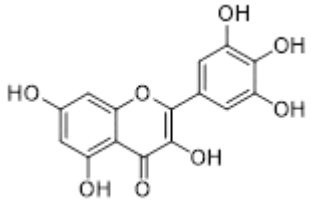 |
| 14 | 5,7-dihydroxy-2-(4-hydroxyphenyl)-4H-chromen-4-one | $C_{15}H_{10}O_5$ | 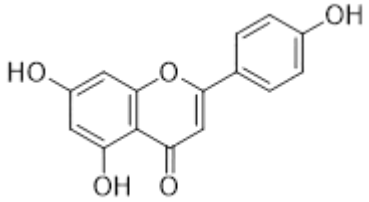 |
| 15 | 3',4',5,7-tetrahydroxyflavone | $C_{15}H_{10}O_6$ | 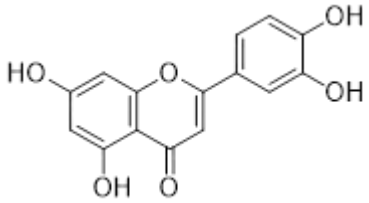 |

## 2.2. Target Protein Selection

Two key therapeutic targets involved in the pathogenesis of rheumatoid arthritis (RA), tumor necrosis factor-alpha (TNF-α) and Janus kinase 3 (JAK3), were selected based on an extensive literature review due to their critical roles in regulating inflammatory signaling pathways. TNF-α is a major pro-inflammatory cytokine responsible for synovial inflammation and joint destruction, whereas JAK3 mediates cytokine-induced signaling through the JAK/STAT pathway, contributing to immune cell activation and disease progression. The three-dimensional crystal structures of TNF-α (PDB ID: 6RMJ) and JAK3 (PDB ID: 3LXK) were retrieved from the Protein Data Bank (PDB) and used for molecular docking studies.(19)

Target Protein 1 (TNF-α): The crystal structure of human tumor necrosis factor-alpha (TNF-α) was retrieved from the Protein Data Bank using PDB ID: 6RMJ.(20) This protein is classified as a cytokine, originates from Homo sapiens, and was expressed in *Escherichia coli* BL21 (DE3). TNF-α plays a central role in mediating inflammatory responses and is one of the primary therapeutic targets in rheumatoid arthritis.(21)

Target Protein 2 (JAK3): The crystal structure of Janus kinase 3 (JAK3) was obtained from the Protein Data Bank using PDB ID: 3LXK. JAK3 is classified as a transferase (protein kinase),(22) is of Homo sapiens origin, and was expressed in *Spodoptera frugiperda*. As a key component of the JAK/STAT signaling pathway, JAK3 regulates cytokine-mediated immune responses and is an important molecular target for developing anti-rheumatoid arthritis agents.(23)

## 2.3. Protein Preparation

The crystal structures of TNF-α (PDB ID: 6RMJ) and JAK3 (PDB ID: 3LXK) were downloaded from the Protein Data Bank (PDB) in PDB format. Before molecular docking, the protein structures were prepared by removing co-crystallized ligands, water molecules, and other non-essential heteroatoms. Missing hydrogen atoms were added, and the protein structures were optimized to obtain suitable receptor conformations for docking analysis.(24) The prepared proteins were subsequently used for molecular docking to evaluate the binding affinity and molecular interactions of the selected compounds.(25)

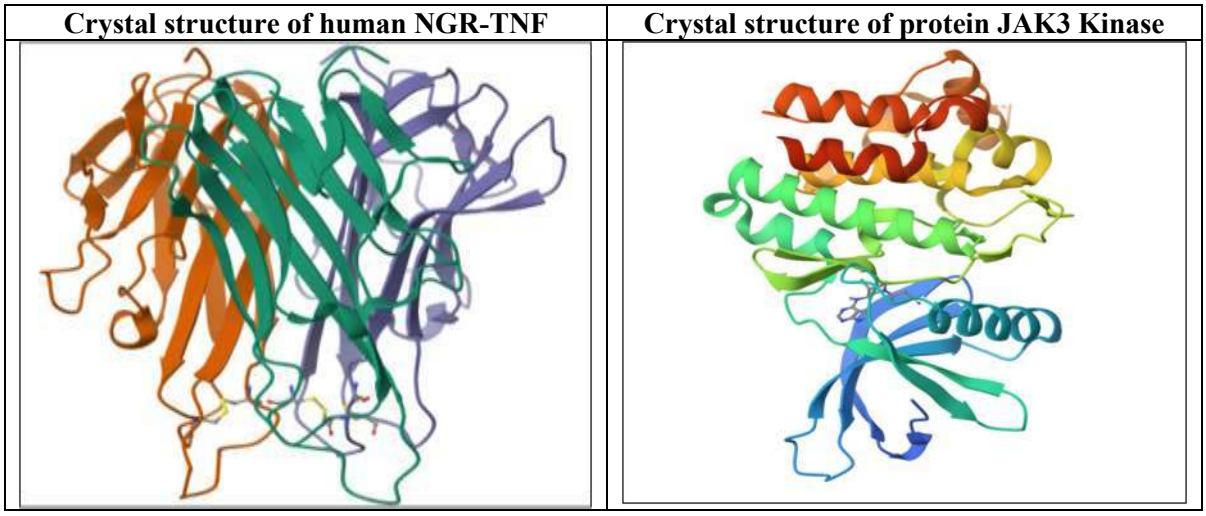


**Figure 1: Crystal structure of human NGR-TNF, Crystal structure of protein JAK3 Kinase**

### 2.4. Ligand preparation

A total of 15 phenolic and flavonoid compounds were selected based on their structural diversity and reported anti-inflammatory potential, identified through an extensive literature survey. The two-dimensional (2D) chemical structures were drawn using ChemDraw and subsequently converted into three-dimensional (3D) structures using Open Babel.(26)(27) The generated 3D conformations were subjected to geometry optimization and energy minimization to obtain stable ligand structures suitable for molecular docking studies. The optimized ligands were then used for subsequent docking analyses against the selected target proteins.(28)

### 2.5 Molecular Docking

Docking studies were conducted using the SwissDock web server, which uses the Dock DSS algorithm to predict binding conformations and estimate the free energy of binding.(29) Each ligand was docked against both 6RMJ and 3LXK to evaluate interaction profiles. The docking findings were studied based on Full Fitness and Estimated ΔG scores, with lower binding energies indicating stronger interactions.(29)(30)

### 2.6 ADME Prediction

The pharmacokinetic properties of the lead compound identified through molecular docking were evaluated using the SwissADME web server. Parameters including absorption, distribution, metabolism, excretion, and drug-likeness were assessed to predict its pharmacokinetic behavior.(31) Physicochemical descriptors such as molecular weight, lipophilicity (LogP), topological polar surface area (TPSA), water solubility, gastrointestinal (GI) absorption, blood–brain barrier (BBB) permeability, P-glycoprotein (P-gp) substrate specificity, cytochrome P450 (CYP) enzyme inhibition, Lipinski's Rule of Five,

bioavailability score, and medicinal chemistry parameters were recorded.(32) These predictions were used to evaluate the compound's suitability as a potential drug candidate.(33)

### 2.7. Toxicity Prediction

The toxicity profile of the lead compound was predicted using the ProTox-II web server. Various toxicity endpoints, including hepatotoxicity, carcinogenicity, mutagenicity, immunotoxicity, cytotoxicity, organ toxicity, Tox21 pathway analysis, molecular initiating events, and cytochrome P450-related toxicity, were evaluated.(34) The predicted toxicity data were used to assess the safety profile and potential toxicological risks of the selected compound before further experimental investigations.(35)

## 3. RESULT AND DISCUSSION

In this study, we explored how fifteen small molecules interact with TNF-α, a key driver of inflammation in rheumatoid arthritis, using molecular docking techniques. Our goal was to assess their potential as inhibitors that could block or weaken this inflammatory signal.

Among the tested compounds, 2-(1-phenylethyl) phenol showed the most promising interaction with TNF-α, reflected by its docking score of −5.86 kcal/mol, which suggests a strong and stable binding. Close behind were 3,4-dimethylphenol (−5.83 kcal/mol) and ortho-benzylphenols (-5.77 kcal/mol), indicating that these molecules may also have inhibitory potential. These results highlight the importance of small hydrophobic groups like methyl or phenylethyl, which seem to improve the molecule's fit within the protein's active site.

On the other hand, some larger or highly polar compounds-especially flavonoid-based structures didn't perform as well. Their docking scores were generally less favorable, ranging between −2.6 and −4.4 kcal/mol. This could be due to their bulkier shapes or the presence of multiple hydroxyl groups, which may hinder their ability to snugly fit into the protein's binding pocket.

Interestingly, one compound -4-methyl-2-(1-phenylethyl) phenol returned an unusually high positive docking score (+24.36 kcal/mol), which typically indicates a failed interaction or docking error. This result was excluded from further interpretation.

Overall, the study suggests that smaller, moderately hydrophobic molecules tend to bind more effectively with TNF-α. These findings provide a useful direction for identifying potential anti-inflammatory drug candidates. In particular, 2-(1-phenylethyl) phenol stands out as a lead compound worthy of further investigation through ADME and toxicity studies to assess its potential as a drug for RA.

The structural analysis of the docked complexes also revealed meaningful insights into how these molecules interact with TNF-α at the molecular level. Most of the effective ligands formed favorable hydrophobic interactions and, in some cases, π-π stacking with key amino acid residues within the binding site. These interactions are essential for stabilizing the ligand-protein complex and could help prevent TNF-α from binding to its receptor. While hydrogen bonding was observed in some cases, it appeared less critical for binding affinity in this particular protein context. These findings not only support the docking scores but also reinforce the relevance of these interactions in guiding structure-based drug design. Taken together, the results highlight a clear direction for selecting and optimizing small-molecule inhibitors with desirable pharmacological profiles for the management of rheumatoid arthritis.

**Table 2. showing SwissParam score for different ligands and protein TNF- alpha Human (NGR-TNF: 6RMJ)**

| Sr. No. | Compounds | SwissParam score |
|---|---|---|
| 1 | ortho-benzylphenols | -5.7776 |
| 2 | 3,4-dimethylphenol | -5.8330 |
| 3 | para-cresol | -5.3754 |
| 4 | 2-(1-phenylethyl) phenol | -5.8594 |
| 5 | 2-methyl-6-(1-phenylethyl) phenol | -3.2531 |
| 6 | 4,5-dimethyl-2-(1-phenylethyl) phenol | -3.2983 |
| 7 | 2-chloro-6-(1-phenylethyl) phenol | -3.8287 |
| 8 | 4-ethyl-2-(1-phenylethyl) phenol | -4.1521 |
| 9 | 4-methyl-2-(1-phenylethyl) phenol | 24.3638 |
| 10 | para-fluorophenol | -5.4987 |
| 11 | ortho-benzylated phenols | -4.4875 |
| 12 | 3,5,7-trihydroxy-2-(4-hydroxyphenyl)-4H-chromen-4-one or 3,4',5,7-tetrahydroxyflavone | -3.3989 |
| 13 | 3,5,7-Trihydroxy-2-(3,4,5-trihydroxyphenyl)-4H-1-benzopyran-4-one | -2.6351 |
| 14 | 5,7-dihydroxy-2-(4-hydroxyphenyl)-4H-chromen-4-one | -3.1233 |
| 15 | 3',4',5,7-tetrahydroxyflavone | -4.4792 |

### 3.1 Comparative Docking Results with 3LXK

Following the promising interactions observed with TNF-α (6RMJ), the same fifteen compounds were docked against a second key RA-related protein target, 3LXK. This structure represents an additional node in the inflammatory signaling network, providing a broader perspective on the inhibitory potential of the compounds.

Interestingly, in contrast to the 6RMJ results, several flavonoid derivatives performed much better with 3LXK. Compounds like 3,5,7-Trihydroxy-2-(3,4,5-trihydroxyphenyl)-4H-1-benzopyran-4-one (−7.04 kcal/mol), 3',4',5,7-tetrahydroxyflavone (−6.93 kcal/mol), and 3,4',5,7-tetrahydroxyflavone (−6.90 kcal/mol) showed significantly improved binding energies compared to their previous interactions with TNF-α. This suggests a more favorable binding pocket or interaction mode in 3LXK for polyhydroxylated scaffolds.

Among phenolic derivatives, 4-methyl-2-(1-phenylethyl) phenol recorded an excellent docking score (−6.79 kcal/mol)—a stark contrast to its anomalous result with TNF-α. Similarly, 4-ethyl-2-(1-phenylethyl) phenol (−6.56 kcal/mol) and ortho-benzylated phenols (−6.50 kcal/mol) also demonstrated strong binding, pointing to a consistent potential across both protein targets.

Notably, the lead compound from the TNF-α study, 2-(1-phenylethyl) phenol, also maintained solid performance here with a docking score of −6.25 kcal/mol, reinforcing its candidacy for further optimization.

**Table 3 showing SwissParam score for different ligands and protein 3LXK**

| Sr. No. | Compounds | SwissParam score |
|---|---|---|
| 1. | ortho-benzylphenols | -6.1609 |
| 2. | 3,4-dimethylphenol | -5.8027 |
| 3. | para-cresol | -5.6925 |
| 4. | 2-(1-phenylethyl) phenol | -6.2508 |
| 5. | 2-methyl-6-(1-phenylethyl) phenol | -6.2196 |

| | | |
|---|---|---|
| 6. | 4,5-dimethyl-2-(1-phenylethyl) phenol | -6.3671 |
| 7. | 2-chloro-6-(1-phenylethyl) phenol | -6.3280 |
| 8. | 4-ethyl-2-(1-phenylethyl) phenol | -6.5628 |
| 9. | 4-methyl-2-(1-phenylethyl) phenol | -6.7965 |
| 10. | para-fluorophenol | -5.6429 |
| 11. | ortho-benzylated phenols | -6.5039 |
| 12. | 3,5,7-trihydroxy-2-(4-hydroxyphenyl)-4H-chromen-4-one or 3,4',5,7-tetrahydroxyflavone | -6.9016 |
| 13. | 3,5,7-Trihydroxy-2-(3,4,5-trihydroxyphenyl)-4H-1-benzopyran-4-one | -7.0449 |
| 14. | 5,7-dihydroxy-2-(4-hydroxyphenyl)-4H-chromen-4-one | -6.7590 |
| 15. | 3',4',5,7-tetrahydroxyflavone | -6.9330 |

### 3.1.1. ortho-benzylphenols

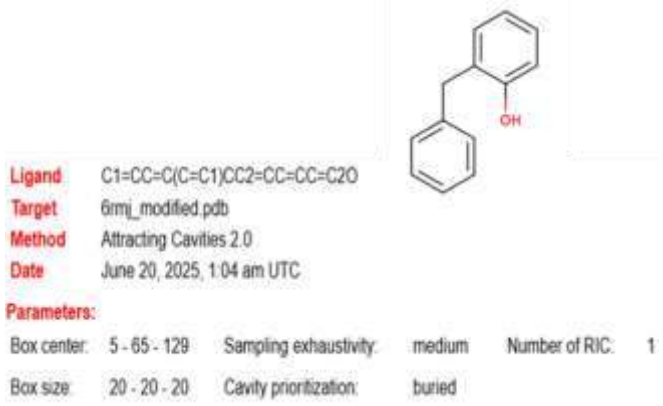


**Figure 2: Chemical structure of ortho-benzylphenols and ligand parameter (box size and center) for target protein 6RMJ**

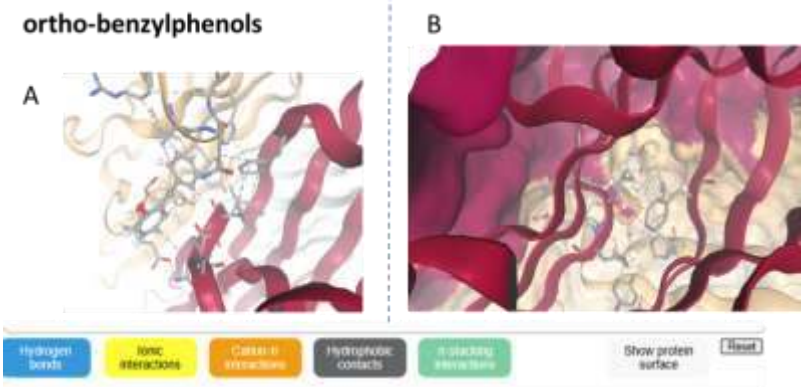


**Figure 3 (A) showing protein (Human TLR2: 1FYW) and ortho-benzylphenols (ligand) interaction and (B) binding pockets along with hydrogen bond ionic interaction, Cation-π interactions, π-stacking interactions, hydrophobic contacts, and protein surface**

**Table 4 showing SwissParam score for ligand ortho-benzylphenols and protein TNF- alpha Human (NGR-TNF: 6RMJ)**

| Cluster number | Cluster member | AC Score | SwissParam Score |
|---|---|---|---|
| 1 | 1 | 7.249793 | -5.7941 |
| 0 | 1 | 6.411049 | -5.7776 |
| 6 | 1 | 9.583450 | 5.7354 |

| | | | |
|---|---|---|---|
| 8 | 1 | 13.341907 | -5.6619 |
| 4 | 1 | 9.097452 | -5.6152 |
| 7 | 1 | 10.313780 | -5.6127 |
| 3 | 1 | 8.321468 | -5.4943 |
| 2 | 1 | 8.570255 | -5.4201 |
| 5 | 1 | 9.559076 | -5.4348 |
| 9 | 1 | 13.792615 | -5.3103 |

### 3.1.2. 3,4-dimethylphenol

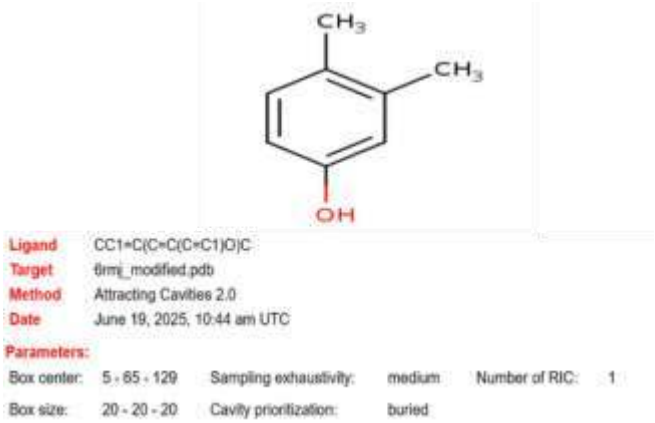


**Figure 4: Chemical structure of 3,4-dimethylphenol and ligand parameter (box size and center) for target protein 6RMJ**

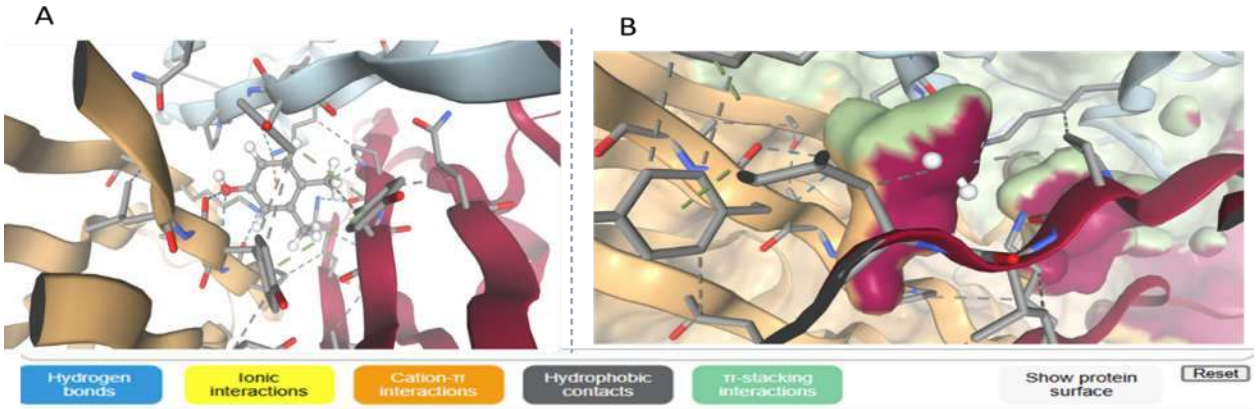


**Figure 5 (A) showing protein (Human TLR2: 1FYW) and 3,4-dimethylphenol (ligand) interaction and (B) binding pockets along with hydrogen bond ionic interaction, Cation-π interactions, π-stacking interactions, hydrophobic contacts, and protein surface**

**Table 5 showing SwissParam score for ligand 3,4-dimethylphenol and protein TNF- alpha Human (NGR-TNF: 6RMJ)**

| Cluster No | Cluster member | AC Score | SwissParam Score |
|---|---|---|---|
| 0 | 1 | -8.713091 | -5.8330 |
| 1 | 1 | -8.504259 | -5.4088 |
| 2 | 1 | -7.670624 | -5.7695 |
| 3 | 1 | -7.532294 | -5.2936 |
| 4 | 1 | -6.321127 | -5.6932 |
| 5 | 1 | -6.027865 | -5.1756 |
| 6 | 1 | -5.616909 | -5.3171 |
| 7 | 1 | -5.515280 | -5.6275 |

| | | | |
|---|---|---|---|
| 8 | 1 | -5.152573 | -5.2640 |
| 9 | 1 | -4.877017 | -5.6252 |

### 3.1.3 para-cresol

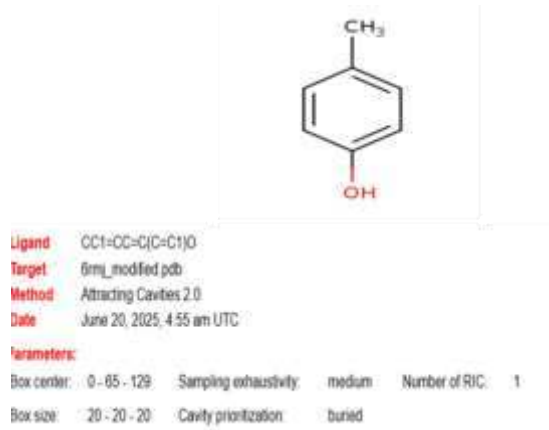


**Figure 6 : Chemical structure of para-cresol and ligand parameter (box size and center) for target protein 6RMJ**

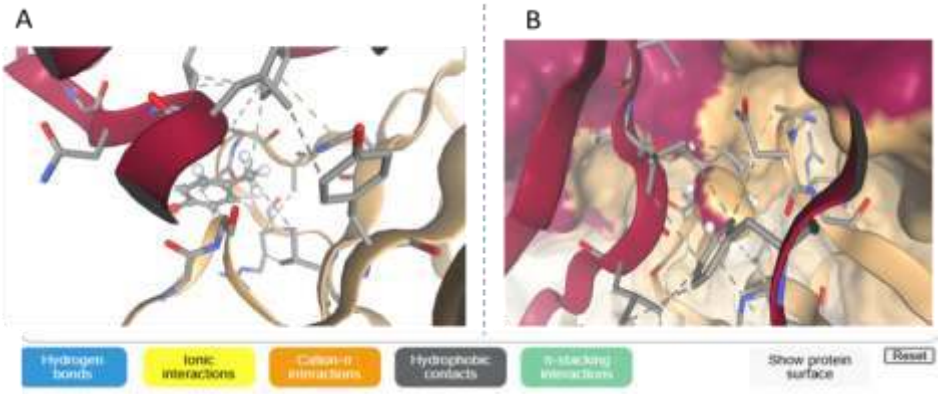


**Figure 7 (A) showing protein (Human TLR2: 1FYW) and para-cresol (ligand) interaction and (B) binding pockets along with hydrogen bond ionic interaction Cation-π interactions, π-stacking interactions, hydrophobic contacts, and protein surface**

**Table 6 showing SwissParam score for ligand para-cresol and protein TNF- alpha Human (NGR-TNF: 6RMJ)**

| Cluster number | Cluster member | AC Score | SwissParam Score |
|---|---|---|---|
| 0.0 | 1.0 | -9.556799 | -5.3754 |
| 1.0 | 1.0 | -9.315639 | -5.3405 |
| 2.0 | 1.0 | -7.423523 | -5.569 |
| 3.0 | 1.0 | -6.698188 | -5.1347 |
| 4.0 | 1.0 | -6.394278 | -5.5149 |
| 5.0 | 1.0 | -5.783588 | -5.493 |
| 6.0 | 1.0 | -5.557225 | -5.4512 |
| 7.0 | 1.0 | -4.940185 | -5.4375 |
| 8.0 | 1.0 | -4.505643 | -4.9206 |
| 9.0 | 1.0 | -3.627285 | -4.9448 |

### 3.1.4 2-(1-phenylethyl) phenol

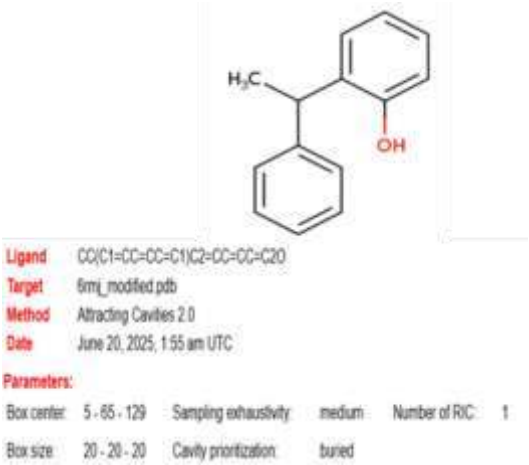


**Figure 8: Chemical structure of 2-(1-phenylethyl) phenol and ligand parameter (box size and center) for target protein 6RMJ**

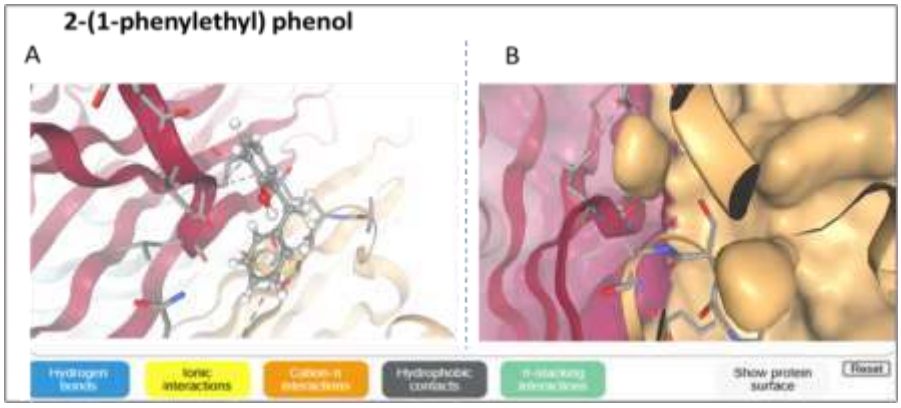


**Figure 9 (A) Showing protein (Human TLR2: 1FYW) and 2-(1-phenylethyl) phenol (ligand) interaction and (B) binding pockets along with hydrogen bond ionic interaction Cation-π interactions, π-stacking interactions, and Hydrophobic contacts and protein surface**

**Table 7 showing swissParam score for ligand 2-(1-phenylethyl) phenol and protein TNF- alpha Human (NGR-TNF: 6RMJ)**

| Cluster number | Cluster member | AC Score | SwissParam Score |
|---|---|---|---|
| 0 | 1 | 8.055628 | -5.8594 |
| 1 | 1 | 9.392927 | -5.5264 |
| 2 | 1 | 9.950115 | -5.8586 |
| 3 | 1 | 10.661143 | -5.5875 |
| 4 | 1 | 12.691628 | -5.6915 |
| 5 | 1 | 12.870985 | -5.6611 |
| 6 | 1 | 12.871569 | -5.4257 |
| 7 | 1 | 14.327294 | -5.5424 |
| 8 | 1 | 14.895088 | -5.4273 |
| 9 | 1 | 16.799977 | -5.3919 |

### 3.1.5 2-methyl-6-(1-phenylethyl) phenol

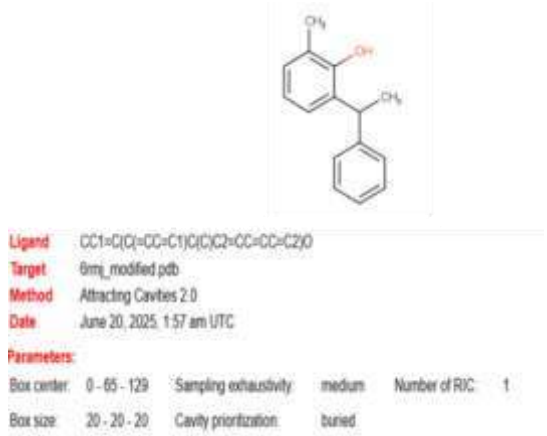


**Figure 10: Chemical structure and ligand parameter (box size and center) for 2-methyl-6-(1-phenylethyl) phenol**

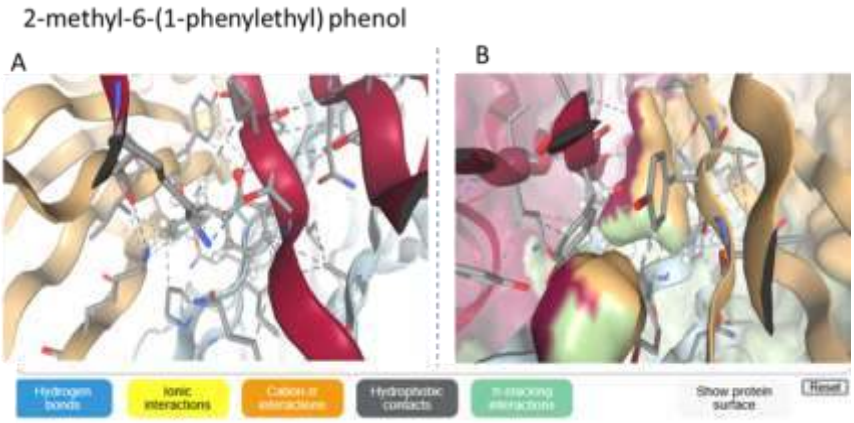


**Figure 11 (A) showing protein (Human TLR2: 1FYW) and 2-methyl-6-(1-phenylethyl) phenol (ligand) interaction and (B) binding pockets along with hydrogen bond ionic interaction Cation-π interactions, π-stacking interactions, hydrophobic contacts and protein surface**

**Table 8 showing swissParam score for ligand 2-methyl-6-(1-phenylethyl) phenol and protein TNF- alpha Human (NGR-TNF: 6RMJ)**

| Cluster number | Cluster member | AC Score | SwissParam Score |
|---|---|---|---|
| 2.0 | 1.0 | 57.726879 | -2.9203 |
| 0.0 | 1.0 | 49.172745 | -3.2531 |
| 8.0 | 1.0 | 105.319922 | -3.2905 |
| 9.0 | 1.0 | 106.786128 | -3.33 |
| 7.0 | 1.0 | 104.43001 | -3.4025 |
| 4.0 | 1.0 | 70.738492 | -3.4087 |
| 3.0 | 1.0 | 58.620039 | -3.4195 |
| 5.0 | 1.0 | 72.440471 | -3.5319 |
| 6.0 | 1.0 | 99.444865 | -3.5801 |
| 1.0 | 1.0 | 55.476893 | -3.829 |

### 3.1.6 4,5-dimethyl-2-(1-phenylethyl) phenol

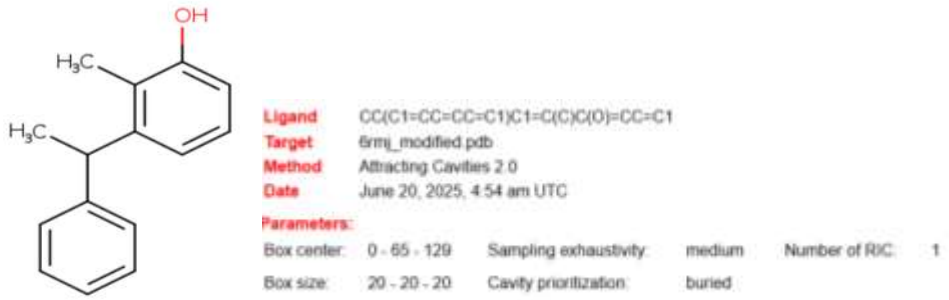


**Figure 12: Chemical structure and ligand parameter (box size and center) for 4,5-dimethyl-2-(1-phenylethyl) phenol**

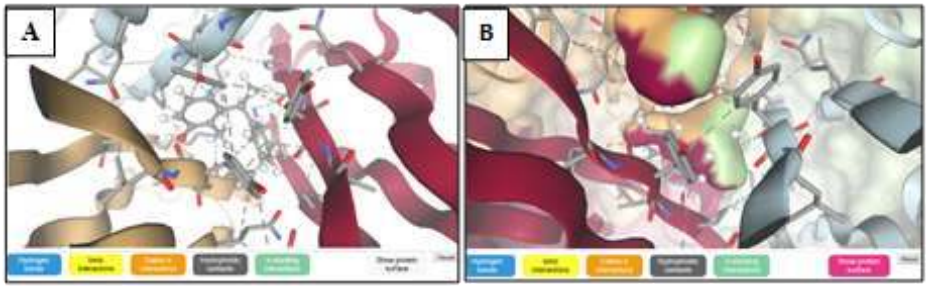


**Figure 13 (A) showing protein (Human TLR2: 1FYW) and 4,5-dimethyl-2-(1-phenylethyl) phenol (ligand) interaction and (B) binding pockets along with hydrogen bond ionic interaction, Cation-π interactions, π-stacking interactions, hydrophobic contacts, and protein surface**

**Table 9 showing swissParam score for ligand 4,5-dimethyl-2-(1-phenylethyl) phenol and protein TNF-alpha Human (NGR-TNF: 6RMJ)**

| Cluster number | Cluster member | AC Score | SwissParam Score |
|---|---|---|---|
| 0 | 1 | 54.212847 | -3.2983 |
| 1 | 1 | 58.968657 | -3.3552 |
| 2 | 1 | 65.053271 | -2.7736 |
| 3 | 1 | 70.83501 | -2.6661 |
| 4 | 1 | 73.119761 | -2.7097 |
| 5 | 1 | 79.271097 | -1.9243 |
| 6 | 1 | 82.446813 | -2.1693 |
| 7 | 1 | 88.304155 | -4.2014 |
| 8 | 1 | 91.754751 | -2.7869 |
| 9 | 1 | 92.004551 | -3.9997 |

### 3.1.7 2-chloro-6-(1-phenylethyl) phenol

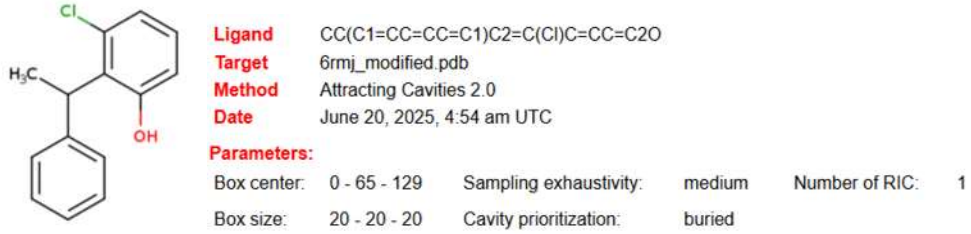


**Figure 14: Chemical structure and ligand parameter (box size and center) for 2-chloro-6-(1-phenylethyl) phenol**

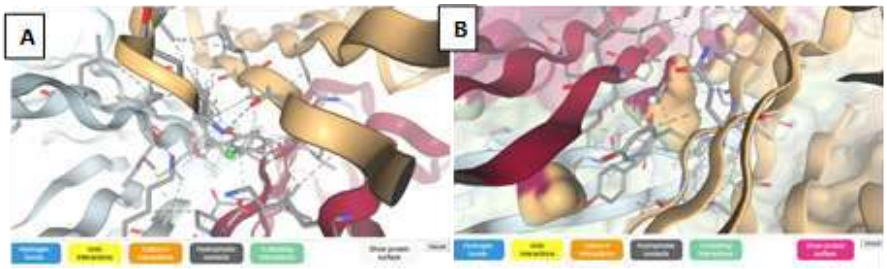


**Figure 19 (A) showing protein (Human TLR2: 1FYW) and 2-chloro-6-(1-phenylethyl) phenol (ligand) interaction, and (B) binding pockets along with hydrogen bond ionic interaction Cation-π interactions, π-stacking interactions, hydrophobic contacts, and protein surface.**

**Table 10 showing swissParam score for ligand 2-chloro-6-(1-phenylethyl) phenol and protein TNF- alpha Human (NGR-TNF: 6RMJ)**

| Cluster number | Cluster member | AC Score | SwissParam Score |
|---|---|---|---|
| 0 | 1 | 42.332487 | -3.8287 |
| 1 | 1 | 49.732148 | -3.214 |
| 2 | 1 | 52.477925 | -3.1348 |
| 3 | 1 | 54.776524 | -3.2208 |
| 4 | 1 | 55.609502 | -3.5752 |
| 5 | 1 | 57.792178 | -3.3635 |
| 6 | 1 | 69.471346 | -4.8191 |
| 7 | 1 | 70.151392 | -2.523 |
| 8 | 1 | 83.122901 | -3.6925 |
| 9 | 1 | 89.078859 | -3.9189 |

### 3.1.8 4-ethyl-2-(1-phenylethyl) phenol

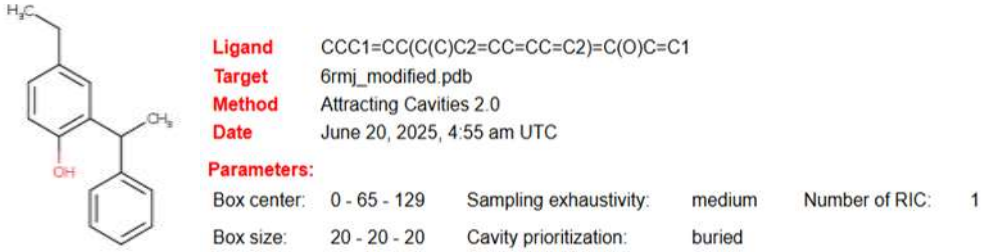


**Figure 15: Chemical structure and ligand parameter (box size and center) for 4-ethyl-2-(1-phenylethyl) phenol**

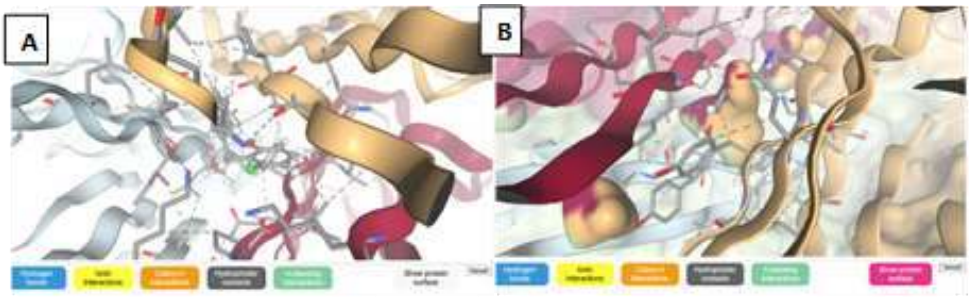


**Figure 16 (A) showing protein (Human TLR2: 1FYW) and 4-ethyl-2-(1-phenylethyl) phenol (ligand) interaction, and (B) binding pockets along with hydrogen bond ionic interaction Cation-π interactions, π-stacking interactions, hydrophobic contacts, and protein surface**

**Table 11 showing swissParam score for ligand 4-ethyl-2-(1-phenylethyl) phenol and protein TNF- alpha Human (NGR-TNF: 6RMJ)**

| Cluster number | Cluster member | AC Score | SwissParam Score |
|---|---|---|---|
| 0 | 1 | 51.493023 | -4.1521 |
| 1 | 1 | 65.267926 | -4.4867 |
| 2 | 1 | 70.320117 | -3.6466 |
| 3 | 1 | 71.345005 | -2.4755 |
| 4 | 1 | 72.163743 | -2.8661 |
| 5 | 1 | 72.318154 | -3.2541 |
| 6 | 1 | 73.181642 | -4.2573 |
| 7 | 1 | 77.099277 | -1.9098 |
| 8 | 1 | 82.975355 | -3.5944 |
| 9 | 1 | 88.564534 | -2.2735 |

### 3.1.9 4-methyl-2-(1-phenylethyl) phenol

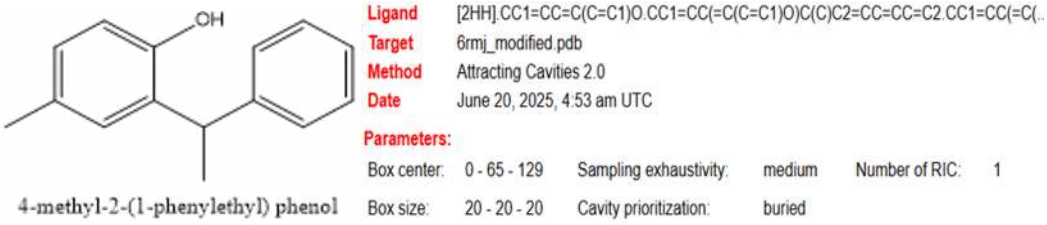


**Figure 17: Chemical structure and ligand parameter (box size and center) for 4-methyl-2-(1-phenylethyl) phenol**

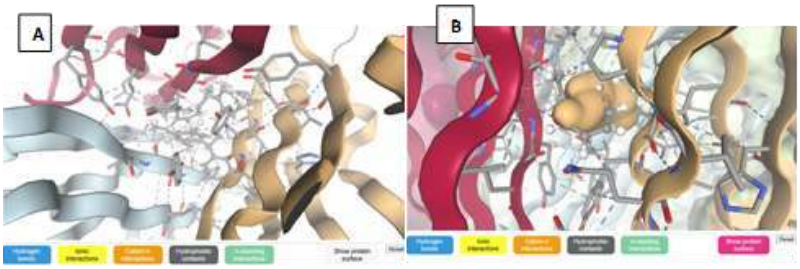


**Figure 18 (A) showing protein (Human TLR2: 1FYW) and 4-methyl-2-(1-phenylethyl) phenol (ligand) interaction, and (B) binding pockets along with hydrogen bond ionic interaction Cation-π interactions, π-stacking interactions, hydrophobic contacts, and protein surface**

**Table 12 showing swissParam score for ligand 4-methyl-2-(1-phenylethyl) phenol and protein TNF- alpha Human (NGR-TNF: 6RMJ)**

| Cluster No | Cluster member | AC Score | SwissParam Score |
|---|---|---|---|
| 0 | 1 | 643.477777 | 24.3638 |
| 1 | 1 | 668.455382 | 24.2305 |
| 2 | 1 | 699.840205 | 26.2609 |
| 3 | 1 | 742.438568 | 28.0442 |
| 4 | 1 | 745.285912 | 22.8377 |
| 5 | 1 | 780.591667 | 24.1875 |
| 6 | 1 | 799.615317 | 29.5397 |
| 7 | 1 | 800.495049 | 30.0234 |
| 8 | 1 | 815.103403 | 24.7583 |
| 9 | 1 | 831.827170 | 29.6598 |

### 3.1.10 para-fluorophenol

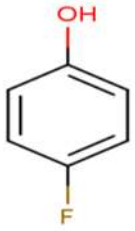


| | |
|---|---|
| Ligand | OC1=CC=C(F)C=C1 |
| Target | 6rmj_modified.pdb |
| Method | Attracting Cavities 2.0 |
| Date | June 20, 2025, 8:09 am UTC |

Parameters:

| | | | | | |
|---|---|---|---|---|---|
| Box center: | 0 - 65 - 129 | Sampling exhaustivity: | medium | Number of RIC: | 1 |
| Box size: | 20 - 20 - 20 | Cavity prioritization: | buried | | |

**Figure 19 : Chemical structure and ligand parameter (box size and center) for para-fluorophenol**

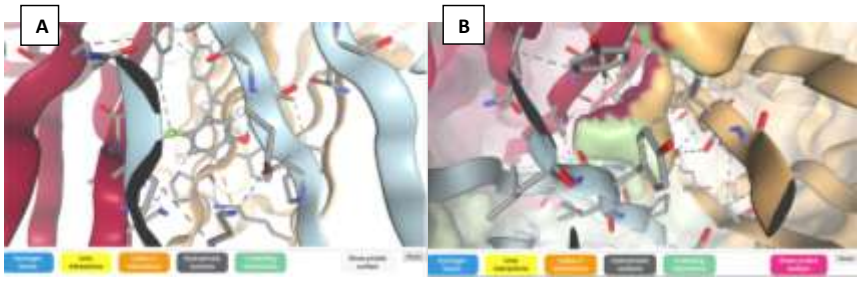


**Figure 20 (A) showing protein (Human TLR2: 1FYW) and para-fluorophenol (ligand) interaction and (B) binding pockets along with hydrogen bond ionic interaction Cation-π interactions, π-stacking interactions, hydrophobic contacts, and protein surface.**

### 3.1.11 ortho-benzylated phenols

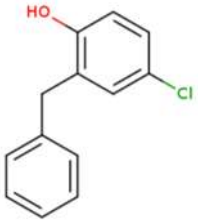


| | |
|---|---|
| Ligand | C1=CC=C(C=C1)CC2=C(C=CC(=C2)Cl)O |
| Target | 6rmj_modified.pdb |
| Method | Attracting Cavities 2.0 |
| Date | June 21, 2025, 1:24 am UTC |

Parameters:

| | | | | | |
|---|---|---|---|---|---|
| Box center: | 0 - 65 - 129 | Sampling exhaustivity: | medium | Number of RIC: | 1 |
| Box size: | 20 - 20 - 20 | Cavity prioritization: | buried | | |

**Figure 21: Chemical structure and ligand parameter (box size and center) for ortho-benzylated phenols**

**Table 13 showing SwissParam score for ligand para-fluorophenol and protein TNF-alpha Human (NGR-TNF: 6RMJ)**

| Cluster No | Cluster member | AC Score | SwissParam Score |
|---|---|---|---|
| 0 | 1 | -7.251124 | -5.4987 |
| 1 | 1 | -6.515236 | -5.4904 |
| 2 | 1 | -5.748955 | -5.4464 |
| 3 | 1 | -5.349590 | -5.3980 |
| 4 | 1 | -4.305113 | -5.3506 |
| 5 | 1 | -3.917207 | -5.3330 |
| 6 | 1 | -2.382805 | -5.1608 |
| 7 | 1 | -1.004561 | -4.7552 |
| 8 | 1 | -0.134212 | -4.6565 |
| 9 | 1 | 0.528482 | -4.8531 |

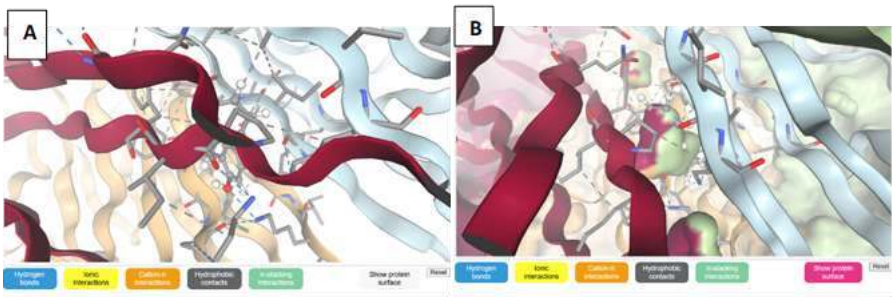


**Figure 22 (A) showing protein (Human TLR2: 1FYW) and ortho-benzylated phenols (ligand) interaction, and (B) binding pockets along with hydrogen bond ionic interaction, Cation-π interactions, π-stacking interactions, and Hydrophobic contacts and protein surface**

**Table 14 showing SwissParam score for ligand ortho-benzylated phenols and protein TNF- alpha Human (NGR-TNF: 6RMJ)**

| Cluster No | Cluster member | AC Score | SwissParam Score |
|---|---|---|---|
| 0 | 1 | 33.965757 | -4.4875 |
| 1 | 1 | 37.470414 | -4.4564 |
| 2 | 1 | 40.786444 | -4.2401 |
| 3 | 1 | 44.009324 | -4.8929 |
| 4 | 1 | 46.020561 | -3.5869 |
| 5 | 1 | 49.737913 | -3.9700 |
| 6 | 1 | 50.611223 | -4.2753 |
| 7 | 1 | 58.686147 | -2.6022 |
| 8 | 1 | 61.990808 | -4.2257 |
| 9 | 1 | 69.773614 | -3.7539 |

### 3.1.12 3,5,7-trihydroxy-2-(4-hydroxyphenyl)-4H-chromen-4-one or 3,4',5,7-tetrahydroxyflavone

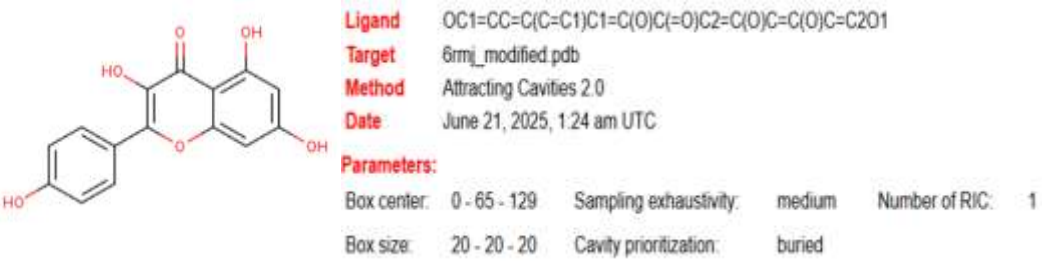


**Figure 23: Chemical structure and ligand parameter (box size and center) for 3,5,7-trihydroxy-2-(4-hydroxyphenyl)-4H-chromen-4-one or 3,4',5,7-tetrahydroxyflavone**

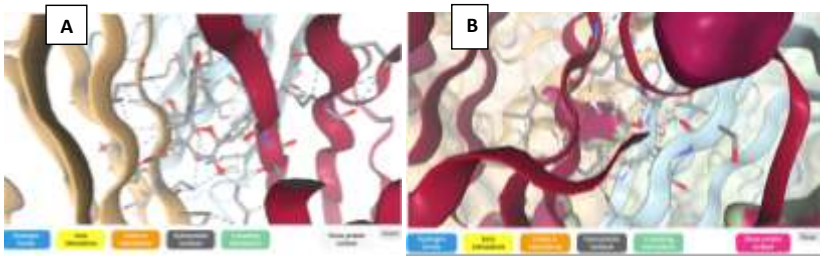


**Figure 24 (A) showing protein (Human TLR2: 1FYW) and 3,5,7-trihydroxy-2-(4-hydroxyphenyl)-4H-chromen-4-one or 3,4',5,7-tetrahydroxyflavone (ligand) interaction and (B) binding pockets along with hydrogen bond ionic interaction Cation-π interactions, π-stacking interactions, and Hydrophobic contacts and protein surface**

**Table 15 showing swissParam score for ligand 3,5,7-trihydroxy-2-(4-hydroxyphenyl)-4H-chromen-4-one or 3,4',5,7-tetrahydroxyflavone and protein TNF- alpha Human (NGR-TNF: 6RMJ)**

| Cluster No | Cluster member | AC Score | SwissParam Score |
|---|---|---|---|
| 0 | 1 | 86.095814 | -3.3989 |
| 1 | 1 | 92.569688 | -2.5853 |
| 2 | 1 | 96.058966 | -3.8817 |
| 3 | 1 | 101.913112 | -4.7263 |
| 4 | 1 | 105.301178 | -2.9073 |
| 5 | 1 | 106.610647 | -2.6551 |
| 6 | 1 | 107.467381 | -3.3174 |
| 7 | 1 | 113.244303 | -2.3824 |
| 8 | 1 | 113.759793 | -2.3417 |
| 9 | 1 | 118.283537 | -3.7444 |

### 3.1.13 3,5,7-Trihydroxy-2-(3,4,5-trihydroxyphenyl)-4H-1-benzopyran-4-one

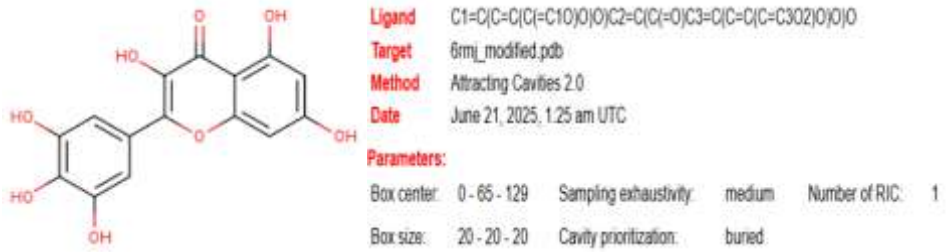


**Figure 25: Chemical structure and ligand parameter (box size and center) for 3,5,7-Trihydroxy-2-(3,4,5-trihydroxyphenyl)-4H-1-benzopyran-4-one**

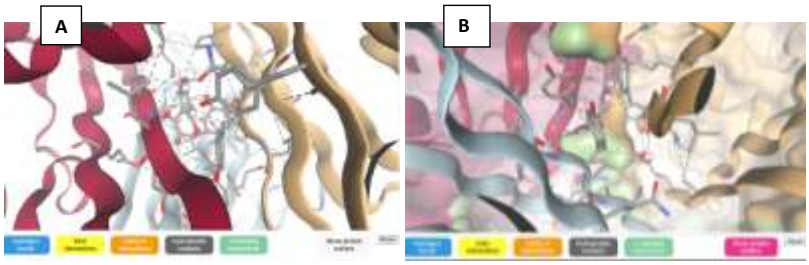


**Figure 26 (A) showing protein (Human TLR2: 1FYW) and 3,5,7-Trihydroxy-2-(3,4,5-trihydroxyphenyl)-4H-1-benzopyran-4-one (ligand) interaction and (B) binding pockets along with hydrogen bond ionic interaction Cation-π interactions, π-stacking interactions, and Hydrophobic contacts and protein surface**

**Table 16 showing swissParam score for ligand 3,5,7-Trihydroxy-2-(3,4,5-trihydroxyphenyl)-4H-1-benzopyran-4-one and protein TNF- alpha Human (NGR-TNF: 6RMJ)**

| Cluster No | Cluster member | AC Score | SwissParam Score |
|---|---|---|---|
| 0 | 1 | 127.597646 | -2.6351 |
| 1 | 1 | 127.988003 | -1.4989 |
| 2 | 1 | 128.230366 | -1.7275 |
| 3 | 1 | 130.389203 | -2.6720 |
| 4 | 1 | 136.344770 | -3.4700 |
| 5 | 1 | 144.701972 | -1.4839 |
| 6 | 1 | 146.035761 | -1.9267 |
| 7 | 1 | 146.243122 | -1.8097 |
| 8 | 1 | 146.922378 | -2.8857 |
| 9 | 1 | 152.504649 | -2.3868 |

### 3.1.14 5,7-dihydroxy-2-(4-hydroxyphenyl)-4H-chromen-4-one

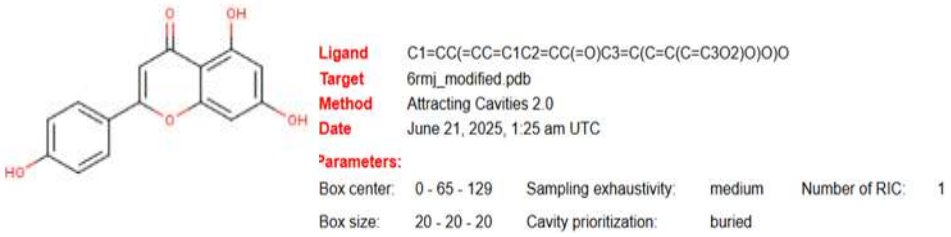


**Figure 27 : Chemical structure and ligand parameter (box size and center) for 5,7-dihydroxy-2-(4-hydroxyphenyl)-4H-chromen-4-one**

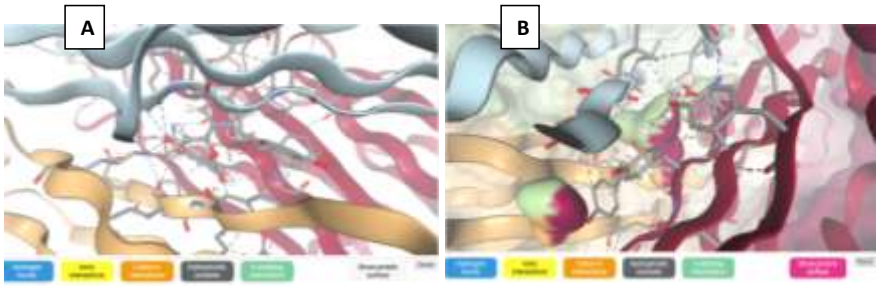


**Figure 28 (A) showing protein (Human TLR2: 1FYW) and 5,7-dihydroxy-2-(4-hydroxyphenyl)-4H-chromen-4-one (ligand) interaction and (B) binding pockets along with hydrogen bond ionic interaction Cation-π interactions, π-stacking interactions, hydrophobic contacts, and protein surface**

**Table 17 showing swissParam score for ligand 5,7-dihydroxy-2-(4-hydroxyphenyl)-4H-chromen-4-one and protein TNF- alpha Human (NGR-TNF: 6RMJ)**

| Cluster No | Cluster member | AC Score | SwissParam Score |
|---|---|---|---|
| 0 | 1 | 63.024515 | -3.1233 |
| 1 | 1 | 66.765651 | -5.3842 |
| 2 | 1 | 69.578492 | -3.4218 |
| 3 | 1 | 73.632933 | -2.8670 |
| 4 | 1 | 75.139970 | -4.0962 |
| 5 | 1 | 75.362864 | -3.2137 |
| 6 | 1 | 80.074656 | -4.8681 |
| 7 | 1 | 80.923665 | -3.6588 |
| 8 | 1 | 83.391234 | -4.1676 |
| 9 | 1 | 93.277709 | -3.0678 |

### 3.1.15 3',4',5,7-tetrahydroxyflavone

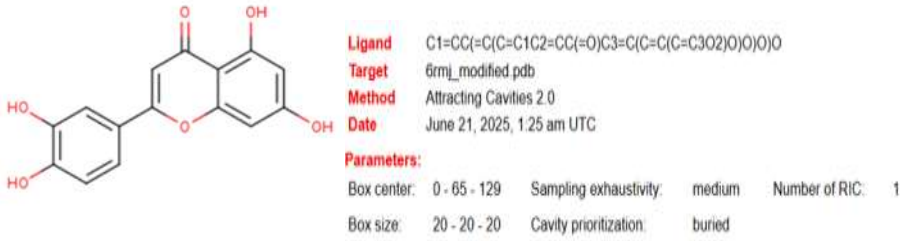


**Figure 29: Chemical structure and ligand parameter (box size and center) for 3',4',5,7-tetrahydroxyflavone**

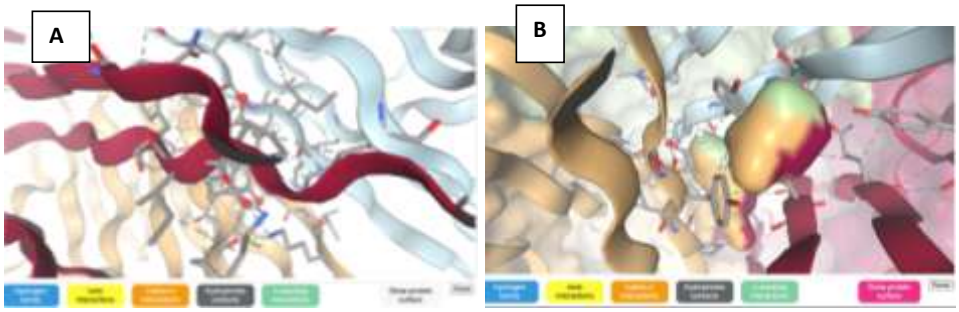


**Figure 30 (A) showing protein (Human TLR2: 1FYW) and 3',4',5,7-tetrahydroxyflavone (ligand) interaction and (B) binding pockets along with hydrogen bond ionic interaction, Cation-π interactions, π-stacking interactions, hydrophobic contacts, and protein surface**

**Table 18 showing SwissParam score for ligand 3',4',5,7-tetrahydroxyflavone and protein TNF- alpha Human (NGR-TNF: 6RMJ)**

| Cluster No | Cluster member | AC Score | SwissParam Score |
|---|---|---|---|
| 0 | 1 | 79.697162 | -4.4792 |
| 1 | 1 | 95.399546 | -2.8890 |
| 2 | 1 | 96.363064 | -2.8291 |
| 3 | 1 | 96.545885 | -2.1009 |
| 4 | 1 | 99.776355 | -3.2367 |
| 5 | 1 | 102.024362 | -2.9480 |
| 6 | 1 | 114.062295 | -1.2139 |
| 7 | 1 | 117.027907 | -1.7194 |
| 8 | 1 | 117.474511 | -2.3601 |
| 9 | 1 | 119.388843 | -2.2041 |

### 3.2 ADME Profiling Prediction:

To evaluate the drug-likeness and pharmacokinetic feasibility of the top-performing compound, a detailed ADME analysis was carried out using SwissADME. The selected molecule (3,5,7-Trihydroxy-2-(3,4,5-trihydroxyphenyl)-4H-1-benzopyran-4-one), with a molecular weight of 318.24 g/mol, falls within an acceptable range for oral bioavailability. However, its topological polar surface area (TPSA) of 151.59 Å² is relatively high, which often correlates with limited passive absorption—a trend reflected in its predicted low gastrointestinal (GI) absorption.

In terms of lipophilicity, the compound exhibits a moderate consensus LogP value of 0.79, suggesting a balanced hydrophilic-lipophilic profile. This can be beneficial for systemic circulation, although the moderate to low predicted skin permeation (Log Kp −7.40 cm/s) indicates minimal transdermal potential. Notably, the compound is predicted not to cross the blood-brain barrier, which is advantageous for targeting peripheral inflammatory conditions like rheumatoid arthritis, as CNS side effects are minimized.

The compound shows favorable water solubility, with all three predictive models (ESOL, Ali, and SILICOS-IT) placing it in the "soluble" category. This supports its potential for formulation in aqueous-based delivery systems. From a metabolic standpoint, the molecule is not a substrate for P-glycoprotein (P-gp), minimizing the risk of efflux-related resistance. However, it may act as an inhibitor of CYP1A2 and CYP3A4, suggesting

that caution is needed when co-administered with drugs metabolized by these enzymes.

From a drug-likeness perspective, the compound adheres to Lipinski's Rule of Five with a single violation (due to its higher number of hydrogen bond donors). It also passes Ghose's filter but fails the Veber, Egan, and Muegge rules, largely due to its high polarity and hydrogen bonding potential. These features, while possibly reducing oral bioavailability, may enhance target specificity in inflammatory conditions.

The bioavailability score of 0.55 suggests moderate systemic exposure if administered orally. Medicinal chemistry filters flagged catechol substructures via both PAINS and Brenk alerts, which are known to sometimes produce false positives in bioassays. Despite this, the compound's synthetic accessibility score of 3.27 indicates a reasonable path toward chemical synthesis and future optimization.

Overall, while some limitations exist—particularly in terms of permeability and enzyme inhibition—this compound presents a structurally promising lead for further refinement, especially as a selective, non-CNS-active JAK3 inhibitor in rheumatoid arthritis therapy.

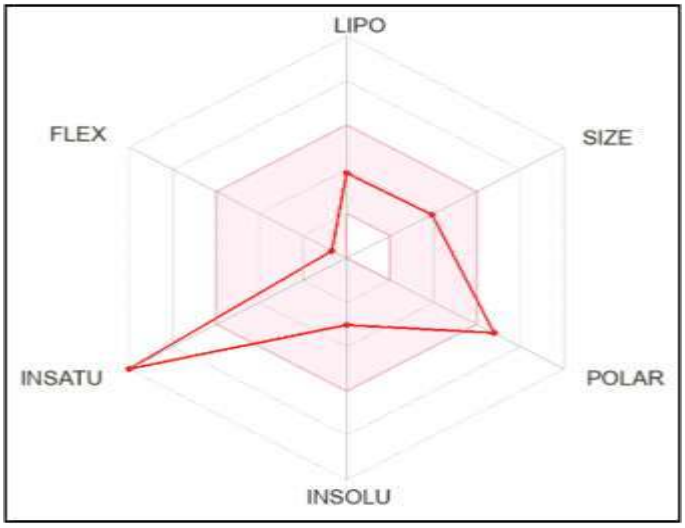


**Figure 31: The color zone is suitable physiochemical space for oral bioavailability**

**Table 19: ADME profile of selected ligand 2-(1-phenylethyl) phenol showing Physicochemical character, Water Solubility, Lipophilicity, Pharmacokinetics, Druglikeness,**

| **Physicochemical Properties** | |
|---|---|
| Formula | C15H10O8 |
| Molecular wt | 318.24 g/mol |
| Aromatic heavy atoms | 16 |
| Fraction Csp3 | 0.00 |
| heavy atoms | 23 |
| Rotatable bonds | 1 |
| Molar Refractivity | 80.06 |
| H-bond acceptors | 8 |
| H-bond donors | 6 |
| TPSA | 151.59 Å² |
| **Lipophilicity** | |
| Log $P_{o/w}$ (iLOGP) | 1.08 |
| **Water Solubility** | |
| Log *S* (ESOL) | -3.01 |

| | |
|---|---|
| Solubility | 3.14e-01 mg/ml; 9.88e-04 mol/l |
| Class | Soluble |
| Log *S* (Ali) | -3.96 |
| Solubility | 3.50e-02 mg/ml; 1.10e-04 mol/l |
| Class | Soluble |
| Log *S* (SILICOS-IT) | -2.66 |
| Solubility | 6.98e-01 mg/ml; 2.19e-03 mol/l |
| Class | Soluble |
| **Pharmacokinetics** | |
| Gastrointestinal absorption | Low |
| BBB permeation | No |
| P-gp substrate | No |
| CYP1A2 inhibitor | Yes |
| CYP2C19 inhibitor | No |
| CYP2C9 inhibitor | No |
| CYP2D6 inhibitor | No |
| CYP3A4 inhibitor | Yes |
| Log $K_p$ (skin permeation) | -7.40 cm/s |
| **Druglikeness** | |
| Lipinski | Yes; 1 violation: NHorOH>5 |
| Ghose | Yes |
| Veber | No; 1 violation: TPSA>140 |
| Egan | No; 1 violation: TPSA>131.6 |
| Muegge | No; 2 violations: TPSA>150, H-don>5 |
| Bioavailability Score | 0.55 |
| **Medicinal Chemistry** | |
| PAINS | 1 alert: catechol_A |
| Brenk | 1 alert: catechol |
| Leadlikeness | Yes |
| Synthetic accessibility | 3.27 |

### 3.3 Toxicity Assessment of the Selected Molecule

To assess the safety and toxicological profile of the lead compound identified through docking—*(3,5,7-Trihydroxy-2-(3,4,5-trihydroxyphenyl)-4H-1-benzopyran-4-one)*—we conducted a detailed prediction using the ProTox-II server. This flavonoid-based molecule, structurally characterized by multiple hydroxyl groups and a polyphenolic backbone, showed a mixed toxicity profile with some areas of concern and others indicating acceptable safety.

From an organ toxicity standpoint, the molecule was predicted to be non-hepatotoxic (probability: 0.69) and non-neurotoxic (0.89), suggesting minimal risk to liver and nervous system tissues. However, nephrotoxicity (0.62) and respiratory toxicity (0.83) were flagged as potential issues. These findings imply a need for focused investigation on renal and pulmonary safety, particularly in chronic administration scenarios.

The model also indicated possible carcinogenic (0.68) and mutagenic (0.51) tendencies, which may be attributed to its polyhydroxylated structure. These alerts do not confirm genotoxicity but suggest that the molecule may influence pathways associated with genomic instability, warranting further experimental assessment.

Importantly, cytotoxicity and immunotoxicity risks were low, with respective probabilities of 0.99 and 0.86 for inactivity. This indicates a reduced likelihood of inducing general cell damage or compromising immune function, reinforcing the compound's potential viability from a systemic toxicity standpoint.

In terms of molecular initiating events and receptor signaling:

- The compound was predicted to activate the aryl hydrocarbon receptor (AhR, 0.91) and both estrogen receptor alpha (ER, 0.87) and its ligand binding domain (ER-LBD, 0.95). These interactions suggest a potential for endocrine disruption, which could be problematic with prolonged exposure.
- On the other hand, no significant interaction was predicted for androgen receptors or PPARγ, which may limit broader hormonal side effects.

From a stress response perspective, activation of mitochondrial membrane potential (MMP) was observed (1.0), raising concerns about mitochondrial health and cellular respiration under drug exposure. However, the compound showed no significant activity on the p53 tumor suppressor or other key stress pathways like ATAD5, HSE, or IS, reducing concern for widespread oxidative or genotoxic stress.

Regarding metabolic enzyme interaction, the molecule showed potential to reduce crucial CYPP450 enzymes such as CYP1A2 (1.0), CYP2C19 (0.77), and CYP2C9 (0.99). This may imply a risk of drug-drug interactions, particularly when co-administered with other substrates metabolized via these pathways. However, it was predicted inactive against CYP3A4, CYP2D6, and CYP2E1, indicating selectivity in its metabolic impact.

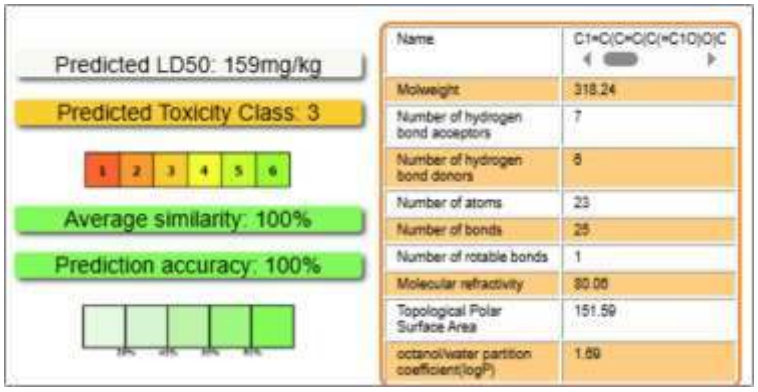


**Figure 32: Oral toxicity prediction results for input compound**

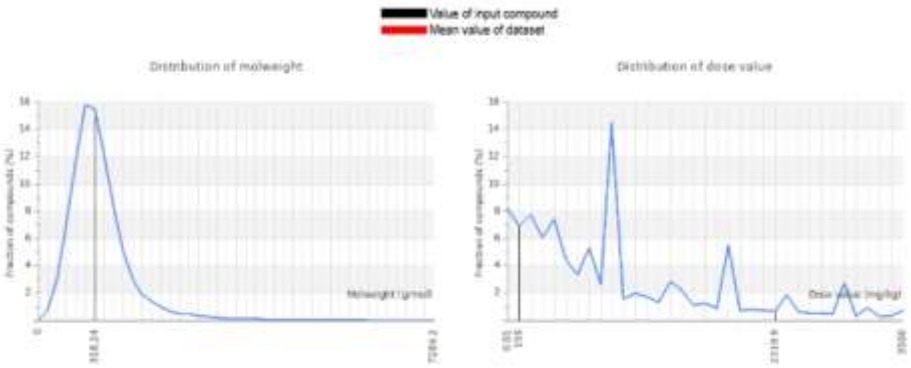


**Figure 33: Comparison of input compound with dataset compounds**

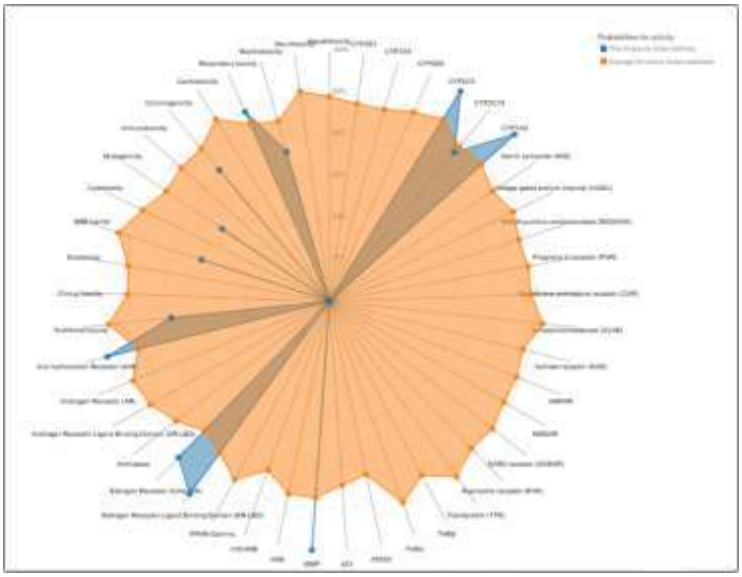

**Figure 34: The toxicity radar chart is to depict the confidence of positive toxicity findings.**

**Table 20: Toxicity Model Report**

| Classification | Target | Prediction | Probability |
|---|---|---|---|
| Organ toxicity | Liver toxicity | -- | 0.69 |
| | Brain toxicity | -- | 0.89 |
| | Kidney toxicity | ++ | 0.62 |
| | Respiratory toxicity | ++ | 0.83 |
| | heart toxicity | -- | 0.99 |
| Toxicity end points | Carcinogenicity | ++ | 0.68 |
| | Immunotoxicity | -- | 0.86 |
| | Mutagenicity | ++ | 0.51 |
| | Cytotoxicity | -- | 0.99 |
| | BBB-barrier | ++ | 0.53 |
| | Ecotoxicity | -- | 0.53 |
| | Clinical toxicity | | 0.53 |
| | Nutritional toxicity | ++ | 0.63 |
| Tox21-Nuclear receptor signalling pathways | Aryl hydrocarbon Receptor (AhR) | ++ | 0.91 |
| | Androgen Receptor (AR) | -- | 0.99 |
| | Androgen Receptor Ligand Binding Domain (AR-LBD) | | 0.97 |
| | Aromatase | | 0.91 |
| | Estrogen Receptor Alpha | ++ | 0.87 |

| | | | |
|---|---|---|---|
| | Estrogen Receptor Ligand Binding Domain (ER-LBD) | | 0.95 |
| | Peroxisome Proliferator Activated Receptor Gamma | -- | 0.98 |
| | Nuclear factor (erythroid-derived 2)-like 2/antioxidant responsive element (nrf2/ARE) | | 0.99 |
| | Heat shock factor response element | | 0.99 |
| | Mitochondrial Membrane Potential | ++ | 1.0 |
| | Phosphoprotein (Tumor Supressor) p53 | -- | 0.97 |
| | ATPase family AAA domain-containing protein 5 | | 0.99 |
| Molecular Initiating Events | Thyroid hormone receptor alpha | | 0.90 |
| | Thyroid hormone receptor beta | | 0.78 |
| | Transtyretrin | | 0.97 |
| | Ryanodine receptor | | 0.98 |
| | GABA receptor | -- | 0.96 |
| | Glutamate N-methyl-D-aspartate receptor | | 0.92 |
| | alpha-amino-3-hydroxy-5-methyl-4-isoxazolepropionate receptor | | 0.97 |
| | Kainate receptor | | 0.99 |
| | Achetylcholinesterase | -- | 0.69 |
| | Constitutive androstane receptor | -- | 0.98 |
| | Pregnane X receptor | | 0.92 |
| | NADH-quinone oxidoreductase | | 0.97 |
| | Voltage gated sodium channel | | 0.95 |
| | Na+/I- symporter (NIS) | | 0.98 |
| Metabolism | CYP1A2 | ++ | 1.0 |
| | CYP2C19 | | 0.77 |
| | CYP2C9 | | 0.99 |
| | CYP2D6 | -- | 0.85 |
| | CYP3A4 | | 0.79 |
| | CYP2E1 | | 1.0 |

**++ denoted active, --denoted as inactive**

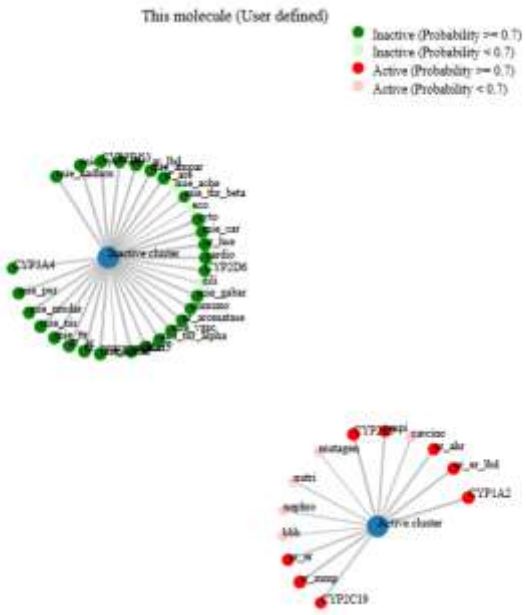


**Figure 35. The network chart to illustrate the connection between the selected compound and predicted activities**

## 4. CONCLUSION

In this study, we explored the potential of selected small molecules as inhibitors of key inflammatory targets involved in rheumatoid arthritis, specifically TNF-α and JAK3. Using molecular docking techniques, we were able to identify several compounds with strong binding affinity, suggesting their ability to interfere with inflammatory signaling. Among them, 2-(1-phenylethyl) phenol emerged as a consistently high performer across both targets, while flavonoid-based compounds showed particular promise in binding effectively to JAK3. To complement the docking results, we carried out ADME and toxicity predictions. These analyses provided insight into the pharmacokinetic behavior and safety profiles of the top candidates. While a few compounds presented limitations such as low predicted oral absorption or potential enzyme inhibition, most showed favorable drug-likeness, solubility, and synthetic accessibility. These findings indicate that the identified molecules hold promise as leads for further development. Altogether, this work lays a solid computational foundation for the design of novel anti-inflammatory agents for rheumatoid arthritis. The results justify advancing the most promising compounds to experimental validation and structural optimization for future therapeutic use.

## REFERENCES


1. Jahid M, Khan KU, Rehan-Ul-Haq, Ahmed RS. Overview of Rheumatoid Arthritis and Scientific Understanding of the Disease. Mediterr J Rheumatol. 2023 Sep;34(3):284–91.
2. Shi W, Liang X, Zhang H, Li H. Burden of rheumatoid arthritis in India from 1990 to 2021: insights from the Global Burden of Disease Database. Front Med. 2025;12:1526218.
3. Masoumi M, Solaymani M, Abbasifard M, Houshmandfar S, Iravani P, Saeedi-Boroujeni A, et al. The genetic puzzle of rheumatoid arthritis: Causes, progression, and treatment. Biochem Biophys Reports [Internet]. 2025 Sep;43:102148. Available from: https://linkinghub.elsevier.com/retrieve/pii/S2405580825002353
4. Anandan M, Narayanan J. Role of T cells and cytokines in the pathogenesis of rheumatoid arthritis. Biochem Biophys Reports. 2025;44:102278.
5. Yap H-Y, Tee SZ-Y, Wong MM-T, Chow S-K, Peh S-C, Teow S-Y. Pathogenic Role of Immune Cells in Rheumatoid Arthritis: Implications in Clinical Treatment and Biomarker Development. Cells. 2018 Oct;7(10).
6. Pei H, He L, Shao M, Yang Z, Ran Y, Li D, et al. Discovery of a highly selective JAK3 inhibitor for the treatment of rheumatoid arthritis. Sci Rep [Internet]. 2018 Mar 27;8(1):5273. Available from: https://www.nature.com/articles/s41598-018-23569-y
7. Ganeshalingam S, Wilson NJ, Ciciriello S, Antonipillai J, Achuthan AA. Cellular interactions in maintaining an inflammatory microenvironment in rheumatoid arthritis. Mol Immunol. 2025;184:112–22.
8. Roodenrijs NMT, Welsing PMJ, van Roon J, Schoneveld JLM, van der Goes MC, Nagy G, et al. Mechanisms underlying DMARD inefficacy in difficult-to-treat rheumatoid arthritis: a narrative review with systematic literature search. Rheumatology. 2022 Sep;61(9):3552–66.
9. dos Santos Nascimento IJ, de Aquino TM, da Silva Júnior EF. Computer-Aided Drug Design of Anti-inflammatory Agents Targeting Microsomal Prostaglandin E 2 Synthase-1 (mPGES-1). Curr Med Chem [Internet]. 2022 Oct;29(33):5397–419. Available from: https://www.eurekaselect.com/202313/article
10. Vijayan S, Margesan T. The potential of Abrus precatorius leaves in arthritis alleviation computational approaches through

lC-MS analysis. Futur Sci OA. 2025 Mar;11:2483131.
11. Kalidass B, Nazeer AA, Mahalingam M, Raja RK, Lakshmanan DK. Exploring the pharmacokinetic, toxicity and anti-arthritic activity of bioactive polyphenols to mitigate the HIF-regulated angiogenic-pannus growth in rheumatoid arthritis. Int Immunopharmacol. 2025;158:114851.
12. Arango JPB, Rodriguez DYM, Cruz SL, Ocampo GT. In silico evaluation of pharmacokinetic properties and molecular docking for the identification of potential anticancer compounds. Comput Biol Chem [Internet]. 2026 Feb;120:108626. Available from: https://linkinghub.elsevier.com/retrieve/pii/S1476927125002877
13. Ancuceanu R, Lascu BE, Dr\uag\uanescu D, Dinu M. In silico ADME methods used in the evaluation of natural products. Pharmaceutics. 2025;17(8):1002.
14. Nakadate K, Ito N, Kawakami K, Yamazaki N. Anti-Inflammatory Actions of Plant-Derived Compounds and Prevention of Chronic Diseases: From Molecular Mechanisms to Applications. Int J Mol Sci. 2025 May;26(11).
15. Saadati F, Modarresi Chahardehi A, Jamshidi N, Jamshidi N, Ghasemi D. Coumarin: A natural solution for alleviating inflammatory disorders. Curr Res Pharmacol drug Discov. 2024;7:100202.
16. Akey KS, Sanapalli BKR, Sigalapalli DK, Tokala R, Sanapalli V. Advancing Drug Repurposing for Rheumatoid Arthritis: Integrating Protein-Protein Interaction, Molecular Docking, and Dynamics Simulations for Targeted Therapeutic Approaches. Curr Issues Mol Biol. 2025 Dec;47(12).
17. Rehman S, Bhatti A, John P. Computational analysis to investigate the anti-rheumatic potential of plant-based small molecule inhibitor targeting tumor necrosis factor α. Front Pharmacol. 2023;14:1127201.
18. Saldívar-González FI, Huerta-García CS, Medina-Franco JL. Chemoinformatics-based enumeration of chemical libraries: a tutorial. J Cheminform [Internet]. 2020 Dec 27;12(1):64. Available from: https://jcheminf.biomedcentral.com/articles/10.1186/s13321-020-00466-z
19. Park JK, Ghang B, Han SW, Ju JH. Current and future treatment of rheumatoid arthritis. J Rheum Dis [Internet]. 2026 Jan 1;33(1):7–18. Available from: http://www.jrd.or.kr/journal/view.html?doi=10.4078/jrd.2025.0034
20. Degano M, Garau G. Crystal structure of human NGR-TNF [Internet]. Worldwide Protein Data Bank. 2019. Available from: https://www.wwpdb.org/pdb?id=pdb_00006rmj
21. Maskos K, Fernandez-Catalan C, Huber R, Bourenkov GP, Bartunik H, Ellestad GA, et al. Crystal structure of the catalytic domain of human tumor necrosis factor-α-converting enzyme. Proc Natl Acad Sci [Internet]. 1998 Mar 31;95(7):3408–12. Available from: https://pnas.org/doi/full/10.1073/pnas.95.7.3408
22. Tan L, Akahane K, McNally R, Reyskens KMSE, Ficarro SB, Liu S, et al. Development of Selective Covalent Janus Kinase 3 Inhibitors. J Med Chem [Internet]. 2015 Aug 27;58(16):6589–606. Available from: https://pubs.acs.org/doi/10.1021/acs.jmedchem.5b00710
23. Pesu M, Laurence A, Kishore N, Zwillich SH, Chan G, O'Shea JJ. Therapeutic targeting of Janus kinases. Immunol Rev [Internet]. 2008 Jun 8;223(1):132–42. Available from: https://onlinelibrary.wiley.com/doi/10.1111/j.1600-065X.2008.00644.x
24. Agu PC, Afiukwa CA, Orji OU, Ezeh EM, Ofoke IH, Ogbu CO, et al. Molecular docking as a tool for the discovery of molecular targets of nutraceuticals in diseases management. Sci Rep [Internet]. 2023 Aug 17;13(1):13398. Available from: https://www.nature.com/articles/s41598-023-40160-2
25. Chrencik JE, Patny A, Leung IK, Korniski B, Emmons TL, Hall T, et al. Structural and Thermodynamic Characterization of the

TYK2 and JAK3 Kinase Domains in Complex with CP-690550 and CMP-6. J Mol Biol [Internet]. 2010 Jul;400(3):413–33. Available from: https://linkinghub.elsevier.com/retrieve/pii/S0022283610004997

26. Karati D, Sen D, Mahanti B, Roy S, Mukherjee S. Computational exploration of novel indanone-pyrazole fused schiff base scaffolds as potential EGFR inhibitors for anticancer therapy. Discov Chem [Internet]. 2026 Feb 10;3(1):67. Available from: https://link.springer.com/10.1007/s44371-026-00503-0
27. Kashyap M, Gupta S, Bansal Y, Bansal G. 2D-QSAR driven design, molecular docking, molecular dynamics simulation and MM/GBSA studies on quinazoline derivatives for development of VEGFR-2 inhibitors. Discov Chem [Internet]. 2025 May 11;2(1):111. Available from: https://link.springer.com/10.1007/s44371-025-00173-4
28. Rashid M, Maqbool A, Shafiq N, Bin Jardan YA, Parveen S, Bourhia M, et al. The combination of multi-approach studies to explore the potential therapeutic mechanisms of imidazole derivatives as an MCF-7 inhibitor in therapeutic strategies. Front Chem [Internet]. 2023 Jun 27;11. Available from: https://www.frontiersin.org/articles/10.3389/fchem.2023.1197665/full
29. Grosdidier A, Zoete V, Michielin O. SwissDock, a protein-small molecule docking web service based on EADock DSS. Nucleic Acids Res [Internet]. 2011 Jul 1;39(suppl):W270–7. Available from: https://academic.oup.com/nar/article-lookup/doi/10.1093/nar/gkr366
30. Röhrig UF, Goullieux M, Bugnon M, Zoete V. Attracting Cavities 2.0: Improving the Flexibility and Robustness for Small-Molecule Docking. J Chem Inf Model [Internet]. 2023 Jun 26;63(12):3925–40. Available from: https://pubs.acs.org/doi/10.1021/acs.jcim.3c00054
31. Odhiambo DO, Omosa LK, Njagi EC, Kithure JG, Wekesa EN. In-silico pharmacokinetics ADME/Tox analysis of phytochemicals from genus Dracaena for their therapeutic potential. Sci African [Internet]. 2025 Sep;29:e02796. Available from: https://linkinghub.elsevier.com/retrieve/pii/S2468227625002650
32. Saritha K, Alivelu M, Mohammad M. Drug-likeness analysis, in silico ADMET profiling of compounds in Kedrostis foetidissima (Jacq.) Cogn, and antibacterial activity of the plant extract. Silico Pharmacol [Internet]. 2024 Jul 19;12(2):67. Available from: https://link.springer.com/10.1007/s40203-024-00240-1
33. Daina A, Michielin O, Zoete V. SwissADME: a free web tool to evaluate pharmacokinetics, drug-likeness and medicinal chemistry friendliness of small molecules. Sci Rep [Internet]. 2017 Mar 3;7(1):42717. Available from: https://www.nature.com/articles/srep42717
34. Banerjee P, Kemmler E, Dunkel M, Preissner R. ProTox 3.0: a webserver for the prediction of toxicity of chemicals. Nucleic Acids Res [Internet]. 2024 Jul 5;52(W1):W513–20. Available from: https://academic.oup.com/nar/article/52/W1/W513/7655780
35. Banerjee P, Eckert AO, Schrey AK, Preissner R. ProTox-II: a webserver for the prediction of toxicity of chemicals. Nucleic Acids Res [Internet]. 2018 Jul 2;46(W1):W257–63. Available from: https://academic.oup.com/nar/article/46/W1/W257/4990033

HOW TO CITE: Ravi Kant Kushwaha, Santosh Kumar Yadav, Alok Saini, Identification of Novel Inhibitors Targeting Inflammatory Pathways in Rheumatoid Arthritis through Drug Design, Computational Docking, and Prediction Studies, Int. J. of Pharm. Sci., 2026, Vol 4, Issue 8, 1747-1774. https://doi.org/10.5281/zenodo.21874491